Check for updates

JGR Space Physics

RESEARCH ARTICLE
10.1029/2022JA030327

Special Section:
The Demonstration and Science Experiment Satellite: Instruments and Mission Overview

Quasi-Periodic Whistler Mode Emission in the Plasmasphere as Observed by the DSX Spacecraft

W. M. Farrell[1], D. S. Lauben[2], J. A. Miller[1,3], U. S. Inan[2,4], I. R. Linscott[2], I. Galkin[5], Y.-J. Su[6], W. R. Johnston[6], M. J. Starks[6], J. C. Sanchez[6], and G. Ginet[7]

[1]NASA/Goddard Space Flight Center, Greenbelt, MD, USA, [2]Stanford University, Stanford, CA, USA, [3]KBR Inc., Houston, TX, USA, [4]Koç University, Istanbul, Turkey, [5]University of Massachusetts at Lowell, Lowell, MA, USA, [6]Air Force Research Laboratory, Kirtland Air Force Base, Albuquerque, NM, USA, [7]MIT/Lincoln Laboratory, Cambridge, MA, USA

Abstract We describe the quasi-periodic (QP) whistler-mode emissions found in the plasmasphere as detected by electric and magnetic instrumentation onboard the Demonstration and Science Experiments (DSX) spacecraft in medium Earth orbit. Over the course of the nearly 2-year mission, at least 45 episodes of whistler mode QP emissions were detected by the Broad Band Receiver (BBR) onboard DSX. Episodes of QP emissions were identified by discrete events having a clear unambiguous periodic nature as detected by both the electric antennae and search coil magnetic sensors in the BBR survey data at 30 s temporal resolution. Most of the QP episodes occurred in a frequency range between 1 and 4 kHz, in a band previously identified by Van Allen Probes and Cluster investigators. However, episodes were also detected by DSX at higher frequencies - events in these episodes extending all the way to 15 kHz. We present our findings on these unusual high frequency events in the presentation herein. Specifically, these high frequency QP episodes tended to be observed near dawn/dusk when the spacecraft was at relatively high magnetic latitudes and on magnetic L-shells between 3 and 5. Another unusual feature of these episodes is that individual up-drifting events making up the episode were found to sometimes occur concurrently in time: The high frequency portion of one up-drifting "polliwog-shaped" event overlapped in time with the low frequency portion of the subsequent event. This behavior of the QP emissions has not been previously emphasized and we consider how this temporal concurrence relates to the source processes.

Plain Language Summary During its nearly 2-year mission, the Demonstration and Science Experiments (DSX) spacecraft detected a number of episodes of medium-altered radio emissions known as "quasi-periodic (QP)" emissions. We show that these emissions are consistent with propagation in the plasma medium in the "whistler mode"—an allowable mode in the plasma medium. In the past, the emission has been described as periodic signal intensifications or drifting bursts typically found between 0.2 and 5 kHz, with the burst periodicity ranging from 10s of seconds to 10s of minutes. We report herein on the DSX observation of a set of QP episodes that extend to frequencies as high as 15 kHz. We also focus our study on QP episodes where the individual bursts appear to overlap in time. This latter characteristic may indicate a source emission region modulated by periodic plasma density waves in the outer plasmasphere.

Key Points:

- We find quasi-periodic (QP) episodes that extend to high frequencies near 15 kHz and have drifting emissions that overlap in time
- The QP emissions having burst overlap points to a possible source modulation by density waves in the plasmasphere
- The measurement set is from a broadband receiver onboard the USAF/Demonstration and Science Experiments spacecraft in medium Earth orbit

Correspondence to:
W. M. Farrell,
farrellbill32@gmail.com

Citation:
Farrell, W. M., Lauben, D. S., Miller, J. A., Inan, U. S., Linscott, I. R., Galkin, I., et al. (2022). Quasi-periodic whistler mode emission in the plasmasphere as observed by the DSX spacecraft. *Journal of Geophysical Research: Space Physics*, *127*, e2022JA030327. https://doi.org/10.1029/2022JA030327

Received 27 JAN 2022
Accepted 27 JUN 2022

Author Contributions:
Conceptualization: U. S. Inan
Data curation: W. R. Johnston, J. C. Sanchez, G. Ginet
Funding acquisition: U. S. Inan, W. R. Johnston, M. J. Starks, J. C. Sanchez, G. Ginet
Investigation: I. Galkin
Methodology: I. Galkin, Y.-J. Su, W. R. Johnston

© 2022 The Authors. This article has been contributed to by U.S. Government employees and their work is in the public domain in the USA.
This is an open access article under the terms of the Creative Commons Attribution License, which permits use, distribution and reproduction in any medium, provided the original work is properly cited.

1. Introduction

We describe the quasi-periodic (QP) whistler-mode emissions detected in the plasmasphere as sensed by electric and magnetic instrumentation onboard the Demonstration and Science Experiments (DSX) spacecraft in medium Earth orbit (MEO). Some of the DSX-observed QP emissions have characteristics that are very similar to those reported previously (i.e., Němec et al., 2018). However, a subset of emissions has unusual morphology that we further describe below.

The presence of quasi-periodic very low frequency (VLF) emissions in the plasmasphere is well-known, detected from both the ground (e.g., Martinez-Calderon et al., 2015a, 2015b, 2016) and from orbital platforms like the Van Allen Probes (e.g., Němec et al., 2018) on field lines that connect through the plasmasphere. The plasmasphere is known to have a whistler-mode "plasmaspheric hiss' that is detected between 200 and ~1 kHz (see the overview by Bortnik, Thorne, and Meredith (2009) and references therein). Episodes of plasmaspheric hiss emission appears as a quasi-continuum in both time and frequency. Episodes of QP emission differ from the plasmaspheric hiss in that they consist of a set of discrete whistler mode bursts, with the bursts quasi-periodically spaced within

21699402, 2022, 8, Downloaded from https://agupubs.onlinelibrary.wiley.com/doi/10.1029/2022JA030327 by Koc University, Wiley Online Library on [03/11/2022]. See the Terms and Conditions (https://onlinelibrary.wiley.com/terms-and-conditions) on Wiley Online Library for rules of use; OA articles are governed by the applicable Creative Commons License

Project Administration: W. R. Johnston, M. J. Starks, J. C. Sanchez, G. Ginet
Resources: U. S. Inan, I. Galkin, Y.-J. Su, M. J. Starks
Software: D. S. Lauben, J. A. Miller, I. Galkin, Y.-J. Su, W. R. Johnston, J. C. Sanchez, G. Ginet
Supervision: D. S. Lauben, U. S. Inan, I. R. Linscott, W. R. Johnston, M. J. Starks, J. C. Sanchez, G. Ginet
Validation: I. R. Linscott
Visualization: D. S. Lauben, J. A. Miller
Writing – review & editing: D. S. Lauben, J. A. Miller, U. S. Inan, I. R. Linscott, I. Galkin, Y.-J. Su, W. R. Johnston, M. J. Starks, J. C. Sanchez, G. Ginet

an episode. The episode can consist of 3 to >20 individual bursts with a spacing between the bursts from 10s of seconds to 10s of minutes (Němec et al., 2013). The frequency extent of the QP emissions is typically between 0.2 and 5 kHz (Hayosh et al., 2014; Němec et al., 2018). However, we present herein QP cases observed by DSX instrumentation that extend up to 15 kHz.

There have been a set of notable recent large-scale studies of QP emission using modern day instrumentation onboard spacecraft in LEO and MEO. In over 27000 orbits, VLF sensing systems onboard the DEMETER spacecraft in LEO commonly detected QP emissions on $L < 6$ on the dayside (QP episodes occurring in about 5% of dayside orbits), but found the emission absent in the nightside (Hayosh et al., 2014). QP emissions were generally found during quiet periods with low Kp, possibly just following a slightly more active period (Hayosh et al., 2013, 2014).

In contrast, plasma wave instruments onboard the Van Allen Probes found QP emissions occurring at all local times within the plasmasphere in a data set spanning 5 years and containing 768 QP episodes (Němec et al., 2018). Therein, they explained the possible difference in high and low altitude local time occurrence as being a propagation effect: QPs generated in the outer plasmasphere ($L \sim 4$) are not able to propagate to low altitudes in the nighttime as demonstrated by previous ray tracing results of Němec et al. (2014) and Martinez-Caldron et al. (2016). However, Němec et al. (2020) reported that the occurrence rate between DEMETER and Van Allen Probes is so strikingly different, especially in local time, that caution has to be used in any comparison between outer plasmasphere and LEO/ground observation sets.

Němec et al. (2018) also reported that the QP emissions as observed by the Van Allen probes were between 0.2 and 4 kHz and had a QP modulation period that extended from <30 s to 12 min, with episode periodicity peaking near 2 min. They noted that there was a mild positive correlation between QP modulation period and local plasmaspheric density. They also took advantage of the baseline made available by the two Van Allen Probe platforms: Two-point measurements between the Van Allen Probes found that the QP region of activity typically spanned about 1.5 hr in local time and 1 Re in radial distance.

Given the large number of spacecraft passing through the plasmasphere, there are now numerous reports of simultaneous observations of the same episodes by different platforms, including the same episodes as observed by the Van Allen Probes, Cluster, and THEMIS (Němec et al., 2016), Van Allen Probes and a ground-based station (Martinez-Calderon et al., 2016), and Cluster and DEMETER (Němec et al., 2013). The simultaneous observations suggest on occasion that the region of QP activity can become very extended in the plasmasphere.

To date, the source of the QP emissions remains unknown. As described by Němec et al. (2018) and references therein, there are two general hypotheses for the generation of the QP episodes: The first concept involves the ULF magnetic wave modulation (i.e., control) of a localized equatorial wave-electron interaction region at the outer edge of the plasmasphere. As described by Coroniti and Kennel (1970) even small changes in the local magnetic field can alter the growth rate of whistlers by creating distortions in velocity phase space of electron distributions. However, a shear or compressional Alfven wave is required to distort B. The second concept for creating QP emissions involves the Flow Cyclotron Instability (Demekhov & Trakhtengerts, 1994) where the pulsation is in association with the expenditure and replenishment of electron free energy in a localized equatorial source region at the outer edge of the plasmasphere. Specifically, in a quasi-ducted equatorial source region at the edge of the plasmasphere, electron free energy could be expended in a local region via the whistler mode instability and thus the source region turns off. The replenishment time (or QP modulation time) reflects the time for a new population of unstable electrons to drift into the source flux tubes and replenish the free energy in the region.

The terrestrial plasmasphere is not the only location where quasi-periodic whistler modes waves are observed. Radio instrumentation onboard the Cassini spacecraft detected quasi-periodic whistler-mode emissions when passing through magnetic field lines near $L \sim 13$ that thread through the outer edge of the Enceladus-sourced plasma torus in Saturn's magnetosphere (Farrell et al., 2017). Radio instrumentation onboard the Juno spacecraft also detected quasi-periodic whistler mode emission when passing near field lines connected to the outer edge of the Io plasma torus in Jupiter's magnetosphere (Hospodarsky et al., 2020). Based on comparative planetology, it appears that the outer edge of equatorial cold plasma regions, where the gradient in density is perpendicular to the magnetic field, may have some common periodic source process.

21699402, 2022, 8, Downloaded from https://agupubs.onlinelibrary.wiley.com/doi/10.1029/2022JA030327 by Koc University, Wiley Online Library on [03/11/2022]. See the Terms and Conditions (https://onlinelibrary.wiley.com/terms-and-conditions) on Wiley Online Library for rules of use; OA articles are governed by the applicable Creative Commons License

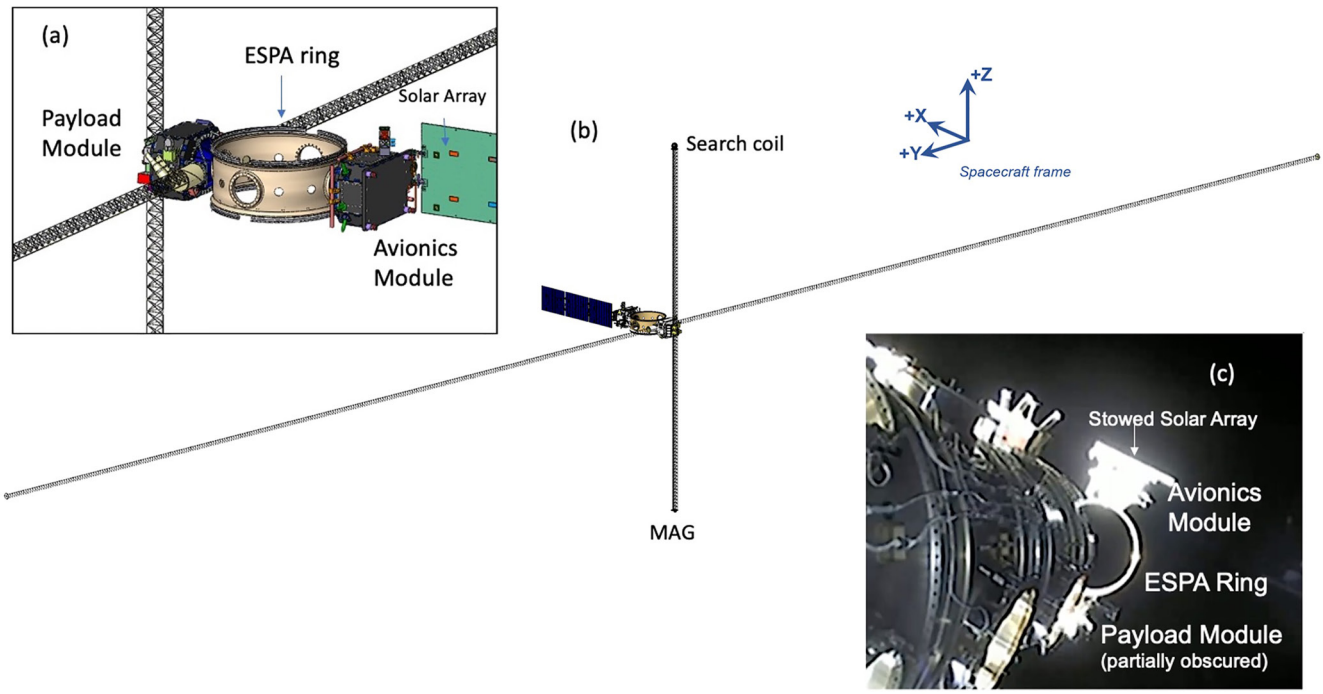


Figure 1. An illustration of the Demonstration and Science Experiments spacecraft shown in its deployed configuration from both (a) a close up and (b) distant perspective, while (c) is an image of the spacecraft at its release from the Falcon Heavy during the STP-2 mission.

We present observations of QP episodes as detected by the VLF electric and magnetic sensors onboard the DSX spacecraft. While many of these QP episodes appear similar in nature to those reported previously, we do find some new and unusual cases worthy of description herein. Specifically, DSX instrumentation detected a subset of QP episodes in the plasmasphere at frequencies between 5 and 15 kHz, which is of higher frequency that the QP episodes reported previously that lie between 0.2 and 5 kHz. As we describe below, some of the bursts in the QP episode were not fully separated in time and overlapped each other. In these cases, individual bursts would appear as up-drifting, polliwog-shaped tones on a spectrogram, with the high frequency portion of one up-drifting tone being ongoing concurrently with the low frequency portion of the next tone. We will discuss this event simultaneity and the implications it might have on the QP burst generation process.

2. The DSX Spacecraft and WPIx System

The Air Force Research Laboratory's DSX spacecraft was launched on 25 June 2019 as part of DoD's Space Test Program-2. The launch was on a SpaceX Falcon Heavy which co-manifested a number of other spacecraft including six COSMIC-2 satellites and a set of cubesats. In total, 24 space vehicles from 13 organizations were launched and delivered into three different orbital ranges. DSX spacecraft operations ceased on 31 May of 2021. The three-axis stabilized DSX spacecraft consists of an avionics module and a payload module both attached to an ESPA ring (Scherbarth et al., 2009; Schoenberg et al., 2006). Figure 1 shows the DSX configuration with (a) a close-up and (b) a distant perspective of the spacecraft with all booms and antenna deployed. Panel (c) shows an image of DSX at the time of separation from the Falcon Heavy booster. The avionics module deployed a solar array while the payload module deployed two 8-m booms (with a magnetometer located at the end of one boom and a search coil located at the end of the other boom), and two 40-m rigid antenna booms (for 81.6-m tip-to-tip distance). See the DSX overview by Johnston et al. (2022) for more details.

DSX was placed in a 2 R_e by 3 R_e (6000 × 12000 km) elliptical orbit with a 42° inclination taking the spacecraft through the plasmasphere, overlapping the inner Van Allen radiation belt and slot region. An objective of DSX was to determine the VLF wave propagation efficiency from ground and space-based transmitters, and to characterize the VLF environment in MEO. Given these objectives, DSX flew a Wave-Particle Interaction Experiment (WPIx) that included (a) a broadband receiver (BBR) built by Stanford University, (b) a tri-axial

21699402, 2022, 8, Downloaded from https://agupubs.onlinelibrary.wiley.com/doi/10.1029/2022JA030327 by Koc University, Wiley Online Library on [03/11/2022]. See the Terms and Conditions (https://onlinelibrary.wiley.com/terms-and-conditions) on Wiley Online Library for rules of use; OA articles are governed by the applicable Creative Commons License

21699402, 2022, 8, Downloaded from https://agupubs.onlinelibrary.wiley.com/doi/10.1029/2022JA030327 by Koc University, Wiley Online Library on [03/11/2022]. See the Terms and Conditions (https://onlinelibrary.wiley.com/terms-and-conditions) on Wiley Online Library for rules of use; OA articles are governed by the applicable Creative Commons License

search coil (TASC) built by NASA/Goddard Space Flight Center, (c) a VLF wave transmitter built by University of Massachusetts at Lowell consisting of a transmitter & tuning unit, narrowband receiver from 3 to 750 kHz, and transmitter control unit (together called TNT), (d) a magnetometer built by UCLA, and (e) a loss cone electron "imager" (LCI) to examine the electrons potentially scattered by wave-particle interactions (see the DSX payload description in Johnston et al., 2022; Scherbarth et al., 2009).

The spacecraft is three-axis stabilized with the spacecraft Z axis aligned with the TASC Boom (see Figure 1b). The X axis of the spacecraft is aligned outward along the solar panel (see also Johnston et al., 2022). We will present survey measurements from the spacecraft Y coordinates (i.e., E_y and B_y). During most passive collection periods like those presented herein, the spacecraft attitude typically cycled in 60 min intervals from sun pointing (15 min) to "cold soak" (45 min) in order to optimize power collection and thermal management. Sun pointing had the +Y axis pointed at the Sun and the Z axis as close as possible to parallel to the Earth's rotation axis. Cold soak shifted the +Y axis from sun pointing by a 60 deg rotation about the Z axis toward the +X axis (Z remaining quasi-parallel to Earth's rotation axis).

The BBR had five input signals: Two E-field inputs between <100 Hz and 50 kHz driven by pre-amplifiers connected to the long 81.6-m rigid dipole antenna (E_y) and an 8-m monopole antenna integrated into the 8-m boom (E_z). There were also three AC magnetic inputs driven by the three search coil 100 Hz–50 kHz pre-amplifiers (B_x, B_y, B_z). These five inputs into the BBR could be switched between five "heritage" 50 kHz receiver channels and five new "micro-receiver" channels. The micro-receiver channels consisted of custom-designed receiver chips that had not been previously operated in the space environment. Each receiver channel included adjustable gains, signal filtering, and additional conditioning. The signal in each of the five channels then underwent analog-to-digital conversion and subsequent onboard spectral analysis, including cross-channel correlations. Survey spectral products of E_y and B_y were produced and consistently returned with a temporal resolution of 30 s. These products will be presented herein. For more details on BBR, see Linscott et al. (2022).

The DSX spacecraft also had the ability to store and return BBR waveform information at 100 kS/s in each of the five channels (0.5 MS/s) in an adjustable time window extending up to 30 min. This waveform capture could occur numerous times per ∼5 hr orbit, with the capture periods pre-programmed based upon ongoing operations, available memory, and discussions with the science team.

3. Plasmaspheric QP Observations

Over the course of the nearly 2-year mission, there were at least 45 episodes of quasi-periodic emissions detected by the BBR. QP emissions were identified as episodes of clear unambiguous periodic events (i.e., broadband bursts or updrift tones) detected by both the electric antenna and search coil magnetic antenna in the survey data. The survey data has a temporal resolution of 30 s, so the QP episodes presented herein typically had events with periodicities greater than 1 min. We note that the DSX detection rate of QP episodes is less than that reported by Němec et al. (2018) using the Van Allen Probes. However, our selection criteria of having both an unambiguous E and B signal together may be a more constraining limit. Of the 45 episodes, about 66% of the these occurred in a frequency range between 1 and 4 kHz in the band described previously by Němec et al. (2018). However, the remaining episodes appeared at higher frequencies extending all the way to 15 kHz.

Figure 2 shows a gallery of frequency versus time spectrograms of QP episodes detected by the B_y sensor of search coil magnetic antenna using the DSX survey measurements. These QP episodes are proto-typical having a periodicity of 1–10 min and a frequency range between about 1 and 4 kHz. Individual events have a spectrogram morphology appearing as "tadpoles" or polliwogs on a frequency versus time spectrogram (especially panel a and c).

While many QP episodes were found between 1 and 4 kHz, a subset of episodes was found at higher frequencies. Figure 3 shows an E_y frequency versus time spectrogram of "polliwog"-shaped QP events occurring on DOY 214 of 2020. This episode lasted for about 75 min and consists of a set of ∼19 up-drifting tones that appear very similar to Figures 2a and 2c, but are now found at higher frequencies between 10 and 15 kHz. The repetition rate for the individual events was about 4 min, but does show variation, with the event occurrence rate slowing to over 10 minutes for the last two events.

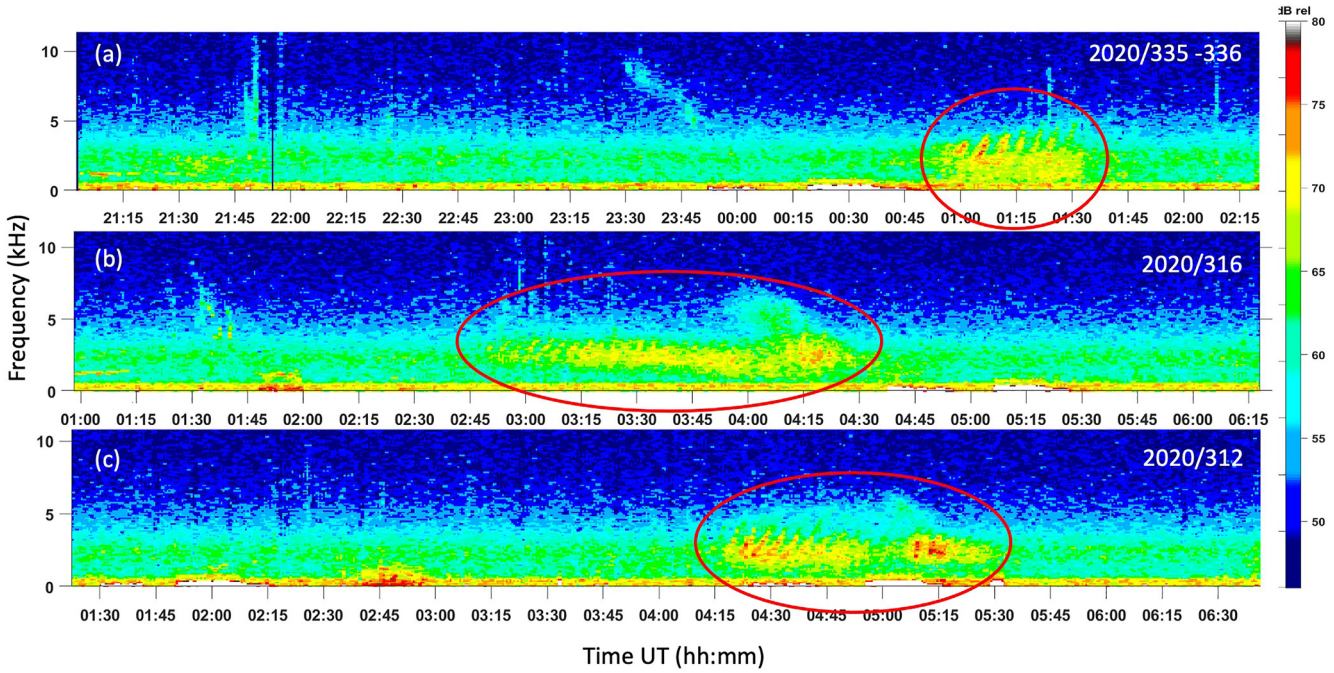


Figure 2. A set of Broad Band Receiver survey frequency versus time spectrograms of quasi-periodic episodes as detected by the magnetic search coil antenna, B_y.

Another interesting feature of this episode is that the individual polliwog up-drifting features can occur concurrently (i.e., overlap in time). The red line in the figure makes this overlap evident. Note that at the same time as the vertical red line, three different up-drifting features are observed simultaneously, with the high frequency portion of one polliwog feature at 14 kHz occurring simultaneously as a 12 kHz emission from the adjacent event and 10 kHz emission from a third event. The QP event displayed in Figure 2c also shows individual up-drifting tones that overlap in time (albeit not as obvious as in Figure 3). This overlap has not been emphasized in previous reports and we will delve into this area further in the discussion section. Figures 4 and 5 shows other examples

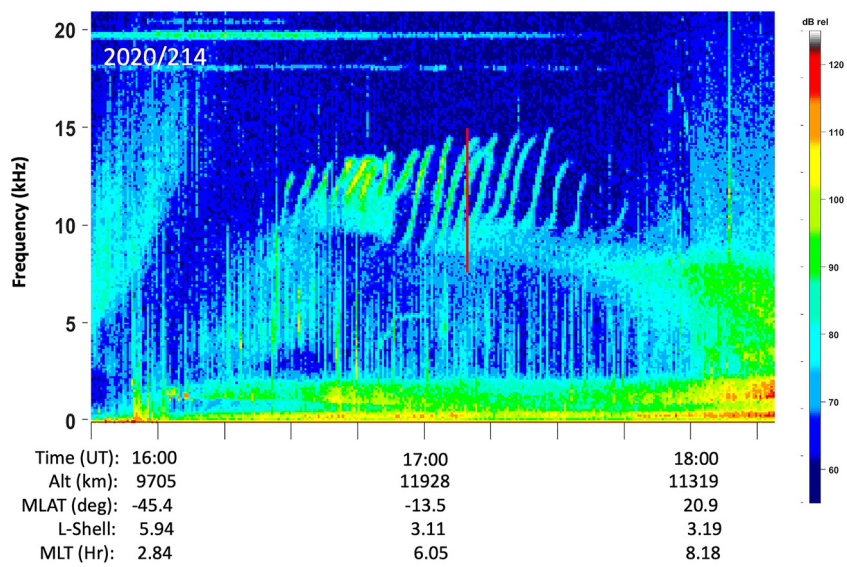


Figure 3. A frequency versus time spectrogram from E_y showing a high frequency quasi-periodic episode having individual up-drifting tones appearing as "polliwog"-shaped features. The tones also overlap slightly in time. During this event, f_{ce} ranged from 55.1 kHz at the event start, to 37.5 kHz in the center of the event, to 40.1 kHz at the end of the event. Unfortunately, there was no TNT narrowband receiver data during the event for a corresponding derivation of f_{UH}.

21699402, 2022, 8, Downloaded from https://agupubs.onlinelibrary.wiley.com/doi/10.1029/2022JA030327 by Koc University, Wiley Online Library on [03/11/2022]. See the Terms and Conditions (https://onlinelibrary.wiley.com/terms-and-conditions) on Wiley Online Library for rules of use; OA articles are governed by the applicable Creative Commons License

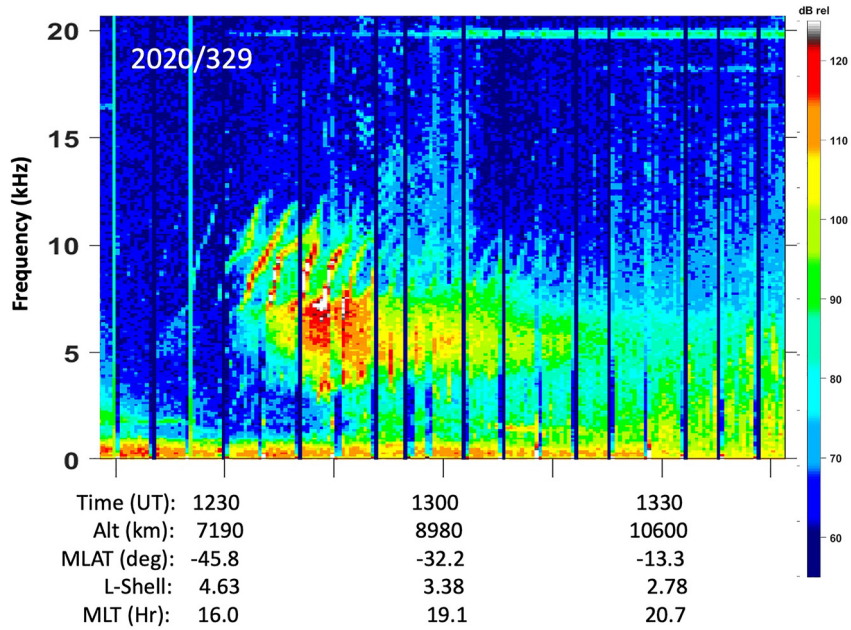


Figure 4. A frequency versus time spectrogram from E_y showing a high frequency quasi-periodic episode. During this event, the value of f_{UH} ranged from 180 kHz at the event start, to 190 kHz in the center of the event, to 250 kHz at the end of the event. The value of f_{ce} ranged from 159.3 kHz at the event start, to 107.6 kHz in the center of the event, to 63.2 kHz at the end of the event.

of the QP episodes occurring above 5 kHz as detected in the electric field, E_y. These episodes also consist of individual polliwog-shaped up-drifting tones that are periodic but updrift such that there is temporal overlap of the features.

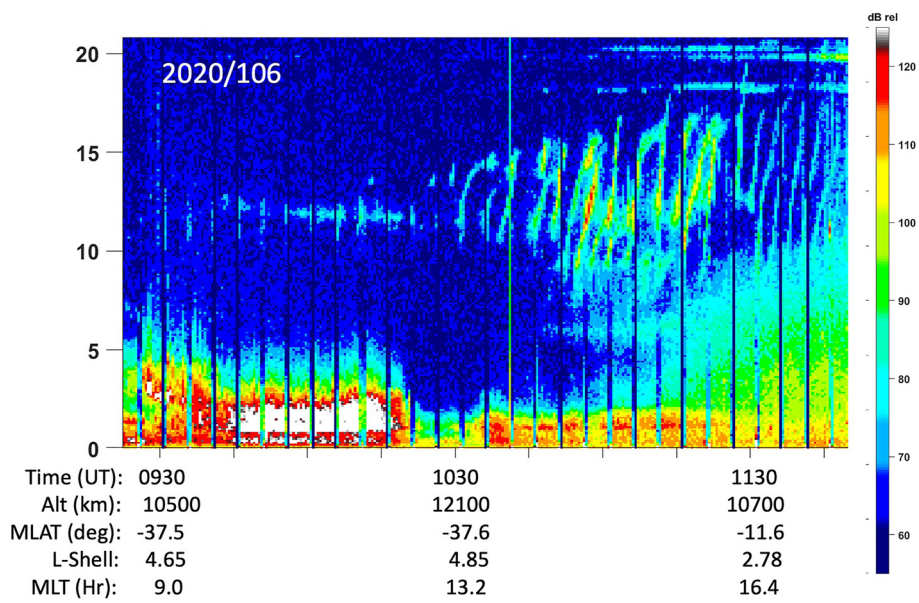


Figure 5. A frequency versus time spectrogram from E_y showing a high frequency quasi-periodic episode. During this event, the value of f_{UH} ranged from 90 kHz at the event start, to 190 kHz in the center of the event, to 300 kHz at the end of the event (see also Figure 7c which displays the TNT narrowband receiver detection of f_{UH} for this same event). The value of f_{ce} ranged from 49.6 kHz at the event start, to 47.3 kHz in the center of the event, to 47.8 kHz at the end of the event.

21699402, 2022, 8, Downloaded from https://agupubs.onlinelibrary.wiley.com/doi/10.1029/2022JA030327 by Koc University, Wiley Online Library on [03/11/2022]. See the Terms and Conditions (https://onlinelibrary.wiley.com/terms-and-conditions) on Wiley Online Library for rules of use; OA articles are governed by the applicable Creative Commons License

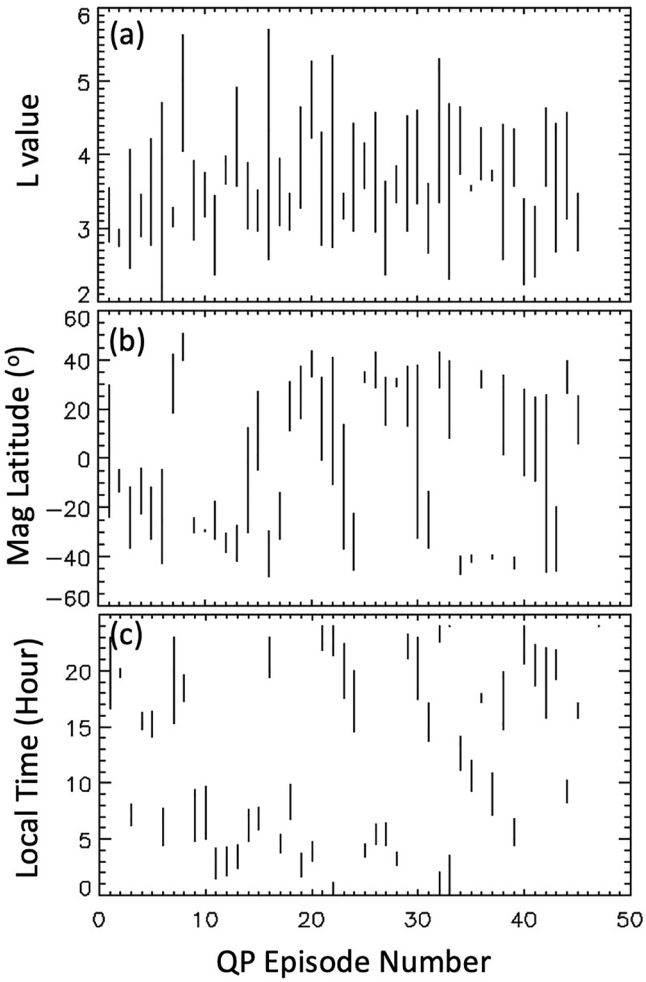


Figure 6. The range of (a) L-shell value, (b) magnetic latitude and (c) local time for the 45 quasi-periodic (QP) episodes found in the Broad Band Receiver (BBR) survey measurements during the Demonstration and Science Experiments (DSX) mission.

Figure 6 shows the episode range of (a) L-shell, (b) magnetic latitude, and (c) local time, respectively, for the 45 QP episodes in the DSX set. Note that the QP episodes are detected in a broad range of L-shells, magnetic latitudes, and local times – including in both dayside and nightside regions examined by DSX. DSX QP observations are thus consistent with Van Allen Probe QP observations, with episodes observed at all LTs (Němec et al., 2018). While the episodes are found in a broad range of locations, there does appear to be a clustering of episodes in LT. For example, note that episodes 40 to 43 all occurred on different orbits but appear near the same range of LT, although the episodes have differing magnetic latitudes ranges from above to below the equator. There is a similar clustering of episodes in LT in pre-dawn hours for the early episodes in the mission. The range of L-shells are found to be broad but having greatest occurrence between an L of 3 and 4.5. Examining Figure 6b, of the 45 episodes, there were only 10 episodes that were detected as DSX transited the magnetic equator. In contrast, there were 32 episodes that were detected predominately at higher magnetic latitudes greater than ± 20°. Thus, while the emissions are found at all latitudes, there is a slight tendency for detection at higher latitudes. We note that the Kp values for nearly all the episodes are relatively low (Daily Kp < 4) except for episode #36 on 25 Jan 2021 (Daily Kp = 5^-) and episode #45 on 20 May 2021 (Daily Kp = 5^+). Consistent with previous studies, we conclude that the QP events are primarily observed during magnetospheric quiet times.

We selected episodes that displayed simultaneous and obvious quasi-periodic activity in both the E-field and B-field sensing systems onboard DSX. Thus, the episodes selected are quasi-electromagnetic in nature. Figure 7 shows the index of refraction characteristics for the event shown in Figure 5, as derived from Appleton-Hartree formalism (Gurnett & Bhattacharjee, 2005). During this episode, DSX is moving from high southern latitudes to low latitudes. As indicated in Figure 7c, the narrowband receiver of TNT detected an upper hybrid frequency, f_{UH}, that was steadily rising from 10:30 to 11:30 UT from ~90 to 300 kHz, while the electron cyclotron frequency, f_{ce}, was just below 50 kHz throughout most of this interval (as determined from a terrestrial dipole magnetic field model). This increase in f_{UH} corresponds to an increasing electron plasma frequency, f_{pe}, from 75 kHz (electron density of ~70/cm^3) at the beginning of the QP episode to 295 kHz (electron density of ~1070/cm^3) at the end of the episode. DSX was thus initially at high southern latitudes crossing relatively high L-shells that are in a lower density region of the plasmasphere, and then moved more equatorward back into the central plasmasphere as the episode was ongoing. We apply a value of $f_{pe} \sim 120$ kHz in our analysis corresponding to the conditions when the QP episode was most intense near 11:00 UT.

In Figure 7a, we find that the whistler mode branch (labeled "W" in the figure) for quasi-parallel propagation has a minimum in index of refraction below a value of 10 between 5 and 15 kHz, which is the same frequency range as the QP episode in Figure 5. As shown in Figure 7b, at 12 kHz, the index of refraction is the lowest at low wave normal angles and becomes large at angles beyond 65°. At these large indices, the emission is considered quasi-electrostatic and a reduction in B-field strength would be expected. Thus, the QP episode having a detectable E and B component is consistent with a whistler mode emission having an index of refraction between 5 and 20.

One immediate consequence of their electromagnetic nature is that the speed of the high frequency QP emission like that in Figure 5 is locally very fast. Thus, the up drifting "polliwog" tones in Figure 3 extending over many minutes are difficult to explain based on a dispersive propagation effect in the plasmasphere. The group velocity for the whistler mode emission in a dense plasma is $v_g \sim 2c\, f^{1/2}\, f_{ce}{}^{1/2} f_{pe}{}^{-1}$ (Gurnett & Bhattacharjee, 2005) which for the QP episode in Figure 5 at 12 kHz corresponds to a value of 0.4c. If the frequency drift is associated with

21699402, 2022, 8, Downloaded from https://agupubs.onlinelibrary.wiley.com/doi/10.1029/2022JA030327 by Koc University, Wiley Online Library on [03/11/2022]. See the Terms and Conditions (https://onlinelibrary.wiley.com/terms-and-conditions) on Wiley Online Library for rules of use; OA articles are governed by the applicable Creative Commons License

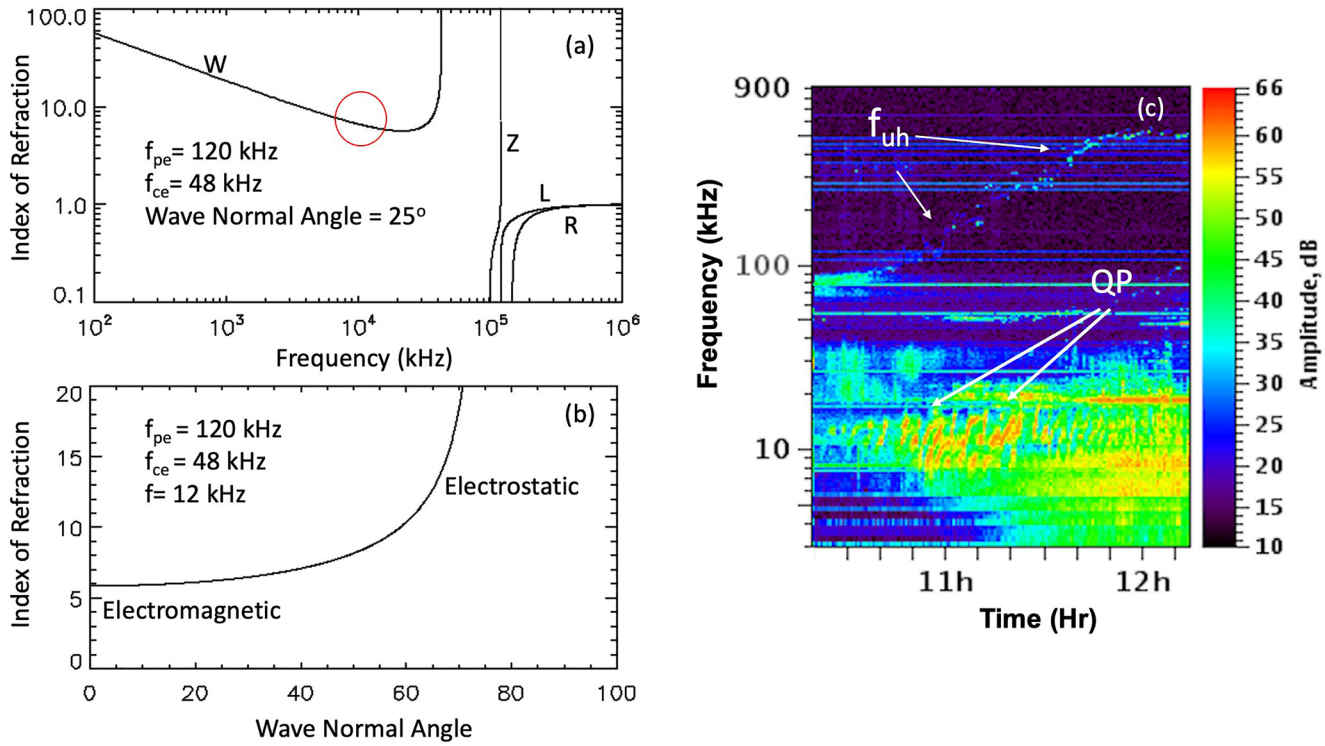


Figure 7. The modeled index of refraction as a function of (a) frequency (at a fixed wave normal angle of 25°) and (b) wave normal angle (as a function of fixed frequency of 12 kHz) run with environmental conditions consistent with the high frequency quasi-periodic (QP) episode shown in Figure 5. Panel (c) shows a TNT Narrowband receiver spectrogram for the event shown in Figure 5, with the QP emission and upper hybrid frequency identified in the figure.

dispersion through the plasmasphere medium, then the distance required to obtain ~4 min of dispersion between 10 and 15 kHz for an individual polliwog feature is over 800 R_e–too long to be realistic. Note also that the group velocity varies directly with $f^{1/2}$, thus higher frequency freely-propagating emissions should arrive at DSX before lower frequency emissions, thus creating to a down-drifting tone (like a VLF lightning whistler). Instead, an up-drifting tone is observed. Hence, we conclude that cutoff-free propagation in the medium can be ruled out to explain the polliwog up-drifting features.

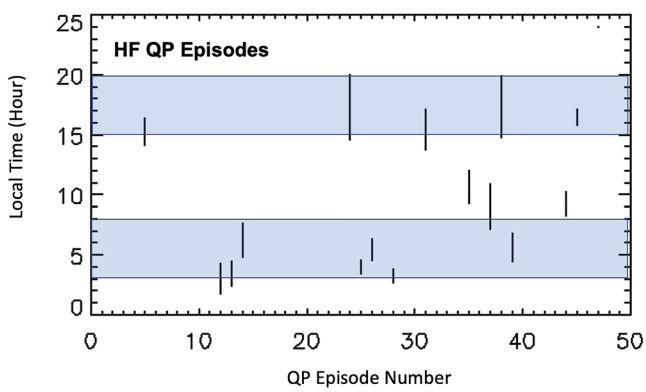


Figure 8. The range of local time for the 15 high frequency quasi-periodic (QP) episodes. These episodes tend to be observed near dawn and dusk.

4. High Frequency QP Episodes

The set of 15 high frequency QP episodes, extending from 5 to 15 kHz, have some common features. First, the episodes tended to be detected at dawn and dusk. Figure 8 shows the local time for the 15 high frequency QP episodes. There is clear clustering of activity with 7 episodes detected between 3 and 8 hr local time and 5 episodes found between 15 and 20 hr local time. Note that only one episode extends to local noon and no high frequency QP activity is detected in the few hours surrounding local midnight.

Second, there is a tendency to observe the high frequency QP episodes when DSX is at relatively high magnetic latitudes. Figure 9 compares (a) location of the center of each of the DSX QP episodes and (b) the same for the subset of high frequency QP episodes. The locations are overlaid on an empirical density model of the plasmasphere derived from IMAGE/RPI observations (Huang et al., 2004). In panel (a), the episodes tend to be located at all latitudes, with the location corresponding to orbital coverage provided by the DSX trajectory. For example, DSX did not extend beyond 3 R_e and consequently activity on L-shell values greater than 3 were only sampled when the spacecraft extended to high latitudes. In panel b, we find that the subset of

21699402, 2022, 8, Downloaded from https://agupubs.onlinelibrary.wiley.com/doi/10.1029/2022JA030327 by Koc University, Wiley Online Library on [03/11/2022]. See the Terms and Conditions (https://onlinelibrary.wiley.com/terms-and-conditions) on Wiley Online Library for rules of use; OA articles are governed by the applicable Creative Commons License

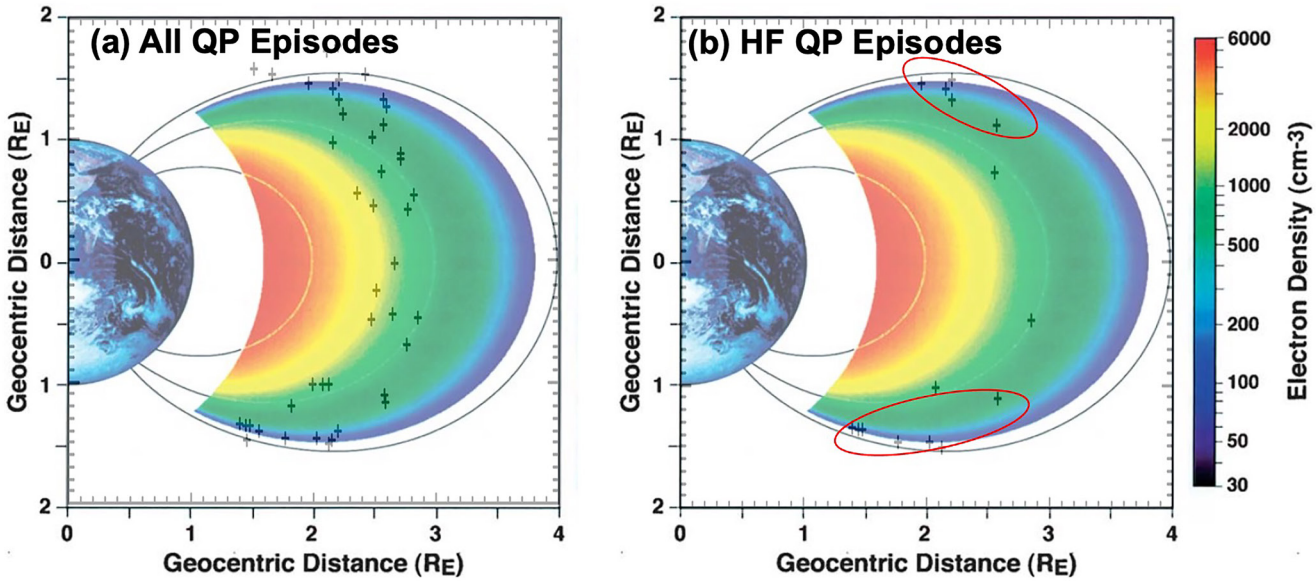


Figure 9. The central location of (a) all quasi-periodic (QP) episodes and (b) the high frequency QP episodes overlaid on an IMAGE/RPI plasmasphere density map from Huang et al. (2004).

high frequency QP episodes tended to be observed when DSX extended to high latitudes on L-shells between 3 and 4.

Third, some of the high frequency QP episodes occurred concurrent with a strong plasmaspheric density gradient as sensed by the change in upper hybrid frequency from the narrowband receiver on TNT (e.g., see Figure 7c). The average position of this gradient is shown in the empirical density model of Figure 9b, with a number of the high frequency QP episode locations (those in the red circle) corresponding to high latitude regions where the plasmaspheric density is quickly changing from <100/cm^3 (blue region) to >500/cm^3 (green region) in a quasi-radial distance of about ~0.25 R_e (~1500 km). However, since the position of the gradient can vary, each episodes needs to be examined in detail to determine if the episode and gradient are concurrent.

Figure 10 shows the range of (a) upper hybrid frequency, f_{UH}, (b) the ratio of the range in f_{uh}, and (c) corresponding density for the 12 episodes that had simultaneous TNT receiver measurements that detected the upper hybrid frequency in the plasmasphere. Most of the QP episodes tended to occur in regions having a broad range in upper hybrid frequency. However, a number of high frequency QP episodes (indicated by asterisk in the figure) tended to occur in low density regions where the upper hybrid emission was below 200 kHz. Parenthetically, there are only 12 high frequency QP events shown, since TNT narrowband receiver measurements were not available for three HF QP cases. Figure 10b shows the ratio of this range in upper hybrid resonance values from the values for each episode shown in Figure 10a. There were four episodes where the upper hybrid frequency changed by a factor of at least 3 during the episode, and all four were high frequency QP episodes.

Using a terrestrial dipole B-field model, a local electron cyclotron frequency was calculated, and an estimate of the density range for each episode was derived (Figure 10c). For locations within 3 R_e and in undisturbed periods, the dipole model provides a reasonable estimate of the magnetic field. Again, most of the QP episodes tended to occur in regions where the density was changing significantly, but 7 of the 12 high frequency QP episodes (those with asterisk) occurred fully or in part at locations where densities dropped below 200/cm^3 during their respective episode. These low densities tended to be found at the beginning or the end of the episode, at a time when DSX was at its largest magnetic latitudes. The typical QP episodes between 1 and 4 kHz (those without asterisk in Figure 10) were also found in a broad range of electron density values but tended to occur in plasmasphere regions with densities above 200/cm^3. For example, of the 24 typical 1–4 kHz QP episodes, only four episodes had part of their emission extending into regions with densities below 200/cm^3. We thus find that there is a general tendency for the high frequency QP emissions to extend into regions having a low density below 200/cm^3.

21699402, 2022, 8, Downloaded from https://agupubs.onlinelibrary.wiley.com/doi/10.1029/2022JA030327 by Koc University, Wiley Online Library on [03/11/2022]. See the Terms and Conditions (https://onlinelibrary.wiley.com/terms-and-conditions) on Wiley Online Library for rules of use; OA articles are governed by the applicable Creative Commons License

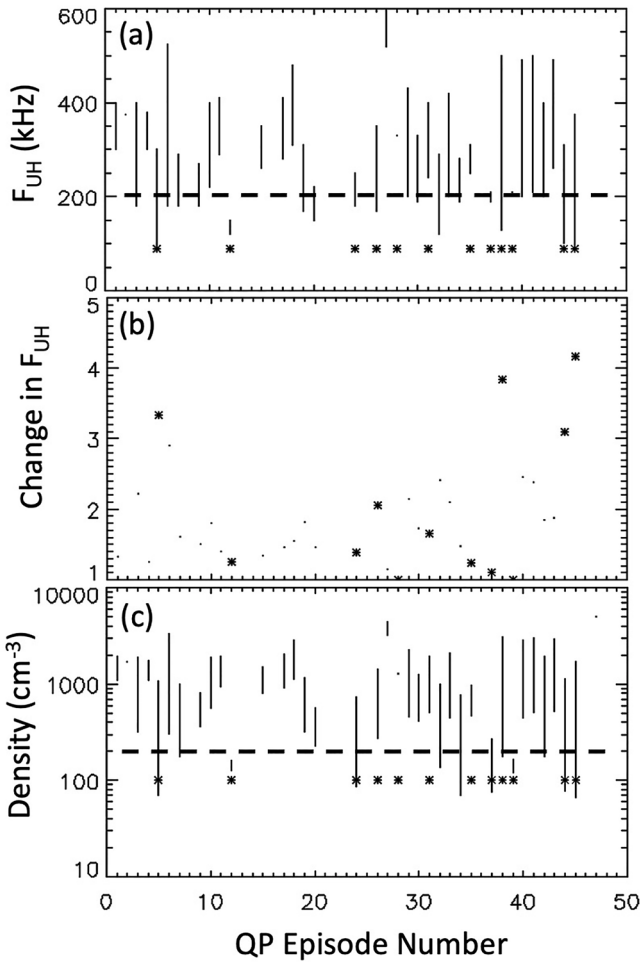


Figure 10. Shown is (a) the range of the upper hybrid frequency during each episode, (b) the ratio of max to min upper hybrid value over that range, and (c) an estimate of the corresponding range in electron density during the episodes. The high frequency quasi-periodic (QP) episodes are identified by asterisk.

5. Discussion

Given these characteristics of the high frequency QP episodes, we can consider possible source processes that could account for the up-drifting polliwog events that can overlap in time. In the past, it has been suggested that ULF magnetic waves may modulate the emission source region to thus control the whistler mode instability and generate the QP emission. Herein, we consider an alternate but related scenario where plasmaspheric density waves act to modulate the whistler mode instability in the QP whistler mode source region. He et al. (2020) reported on the observation of plasmasphere density wave activity occurring during a solar storm that gives rise to a saw-tooth aurora and drives ULF magnetic waves. While the high frequency QP emissions presented herein occur during relatively low Kp periods, electron density modulations are frequently occurring throughout the outer plasmasphere (see Figures 9 and 10 of LeDocq et al., 1994). CRRES detected quasi-periodic density fluctuations with density variations up to 200/cm^3 in a frequency range in the spacecraft frame from 2 mHz (~8 min) to 61 mHz (~0.25 min) (LeDocq et al., 1994). Given that the electron resonance energy for the whistler mode instability varies as $1/n_e$ (Gurnett & Bhattacharjee, 2005), a modulation by a small factor in density in the source region can shift the growing whistler waves out of resonance with a stable energetic electron population in the source region. For example, Gary and Wang (1996) found that the threshold for initiation of the whistler mode instability is a function of plasma β (and density), and thus could be controlled by a density wave. A quasi-periodic wave-like density modulation would then take a source region repeatedly in and out of resonance with a stable energetic electron population, giving rise to a quasi-periodic emission.

Thus, one non-unique interpretation of the up-drifting polliwog events found in each episode is that they are associated with a cold plasma density wave propagating through an equator whistler mode source region, as illustrated in Figure 11. In the source region, we presume that the emission source at each frequency would be displaced spatially, with low frequency emission coming from a region at larger radial distance and high frequency region at lower radial distance. As the density wave propagates through the source region, it stimulates emission at a given location and frequency when the density in the wave is of the correct value to maximize the electron resonance with the whistler mode waves. Each up-drifting tone then represents a density modulation propagating through the source region as it progressively stimulates growth at each source location. In the illustration, there are two density modulations in the source region, A and B. Modulation B is located at lower L-shell and emitting at a higher frequency than the emission generated at the location of modulation A. As both density modulations propagate through the source region, they create the up-drifting tones. As illustrated, if the density modulation separation (i.e., wavelength) is less than the size of the source region, then multiple density modulations can be contained in the source region, giving rise to temporally concurrent up-drifting tones. Specifically, the high frequency emission from one source location triggered by density modulation B occurs at the same time as the low frequency emission from another source location triggered by density modulation A. As shown in Figure 7, the low index of refraction suggests the waves are propagating at high speeds and thus the quasi-periodic nature of the emission is assumed to be connected directly to the density modulation in the source region and is not associated with a propagation effect. However, this cannot be stated with certainty. Thus, in the future, a ray tracing analysis should be performed to determine the density wave's effect in the source and along the field line on propagation. We also note that this density modulation model may also be applicable to the QP emissions between 1 and 4 kHz, although we cannot rule out other possible scenarios as well (i.e., the model is non-unique). We thus present a high-level description of a density modulation model herein and future work will include a more detailed analysis (i.e., raytracing, analysis of possible source properties etc.).

21699402, 2022, 8, Downloaded from https://agupubs.onlinelibrary.wiley.com/doi/10.1029/2022JA030327 by Koc University, Wiley Online Library on [03/11/2022]. See the Terms and Conditions (https://onlinelibrary.wiley.com/terms-and-conditions) on Wiley Online Library for rules of use; OA articles are governed by the applicable Creative Commons License

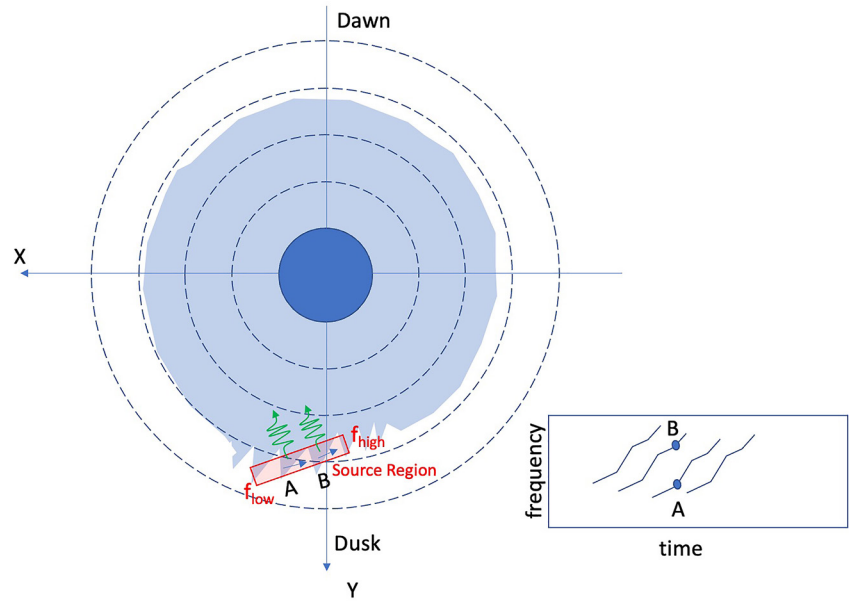


Figure 11. Cartoon illustration of a density wave passing through a quasi-periodic source region. Assuming a continuous energetic electron population, the cold electron density modulations takes the energetic electron population in and out of resonance with the whistler mode waves. The modulations, like A and B, traveling through the source region gives rise to the up-drifting features. See text for more details. Illustration of the plasmasphere and density wave is adapted from He et al. (2020).

One can envision other variations on this density concept but, in each case, the fluctuation in density would be the controlling element giving rise to the QP emission. Unfortunately, DSX spatial coverage is limited in equatorial regions to <3 R_e and thus we do not have a direct sense of the outer plasmasphere conditions at the equator that might magnetically-connect to the high latitude, high frequency QP episodes at or beyond L ~ 4.

However, there is a second compelling source scenario for QP emissions. Bortnik et al. (2008) and Bortnik, Li, et al. (2009) presented the interesting possibility that extra-plasmaspheric chorus can propagate into the plasmasphere, entering at high latitudes near L ~ 3–4 to thus become part of the plasmaspheric hiss emissions. Figure 1 of Bortnik et al. (2008) shows the ray paths of chorus launched near L = 6 from an equatorial source, the entry of chorus into the plasmasphere at high latitudes, and the subsequent trapped ray within the plasmasphere. While that study emphasized signals near 1 kHz, an analogous scenario could be made for the high frequency QP emissions discussed herein. As indicated in Figure 9, DSX's high latitude excursions may have allowed the spacecraft to pass through the entry region for extra-plasmaspheric chorus. Chorus is also known to be present at high frequencies (5–15 kHz), further connecting these high frequency QP episodes to chorus. However, an argument against this second model is that the source region for such a high frequency emission would lie on L-shells below 4, placing the source inside the plasmasphere. Chorus also consists of up-drifting tones but on substantially shorter time-scales–10s of milliseconds. Further study is needed to determine if the wave dispersion is so great upon entering the high density plasmaspheric region that the chorus up-drifting tones can dilate to minute time-scales. The low index of refraction (Figure 7) suggests that such dilation is extremely difficult to envision in the middle plasmasphere, but the refraction of emission at the high latitude entry point may provide event dilation. While an interesting model, this scenario may not completely fit the high frequency QP bursts but still could explain the lower frequency QP emissions between 1 and 4 kHz.

It should be noted that two of the high frequency QP episodes were detected in a low-density region immediately adjacent to a very steep high-density region. In Figure 11, these are episodes 12 and 39. Note that the upper hybrid frequency and derived electron density in these three cases did not display a large range since the waves did not appear to propagate into the steep density gradient region. One possible (non-unique) interpretation of these episodes in the Bortnik et al. (2008), Bortnik, Li, et al. (2009) is that the density gradient was so steep that the extra-plasmaspheric chorus was refracted away from the plasmasphere, and thus could not enter at this time.

21699402, 2022, 8, Downloaded from https://agupubs.onlinelibrary.wiley.com/doi/10.1029/2022JA030327 by Koc University, Wiley Online Library on [03/11/2022]. See the Terms and Conditions (https://onlinelibrary.wiley.com/terms-and-conditions) on Wiley Online Library for rules of use; OA articles are governed by the applicable Creative Commons License

21699402, 2022, 8, Downloaded from https://agupubs.onlinelibrary.wiley.com/doi/10.1029/2022JA030327 by Koc University, Wiley Online Library on [03/11/2022]. See the Terms and Conditions (https://onlinelibrary.wiley.com/terms-and-conditions) on Wiley Online Library for rules of use; OA articles are governed by the applicable Creative Commons License

In contrast, for other episodes, the chorus could enter at high latitudes to thus ultimately appear as the high frequency QP emissions.

Further study is needed to fully understand the source of these high frequency QP episodes (and, in general, all of the QP episodes). Such studies should pursue the connection of the QP emissions to plasmaspheric density modulations. While we emphasize the observations herein, future studies using ray tracing should occur to understand the effect of the gradient on QP source and propagation.

6. Conclusions

We present new findings associated with plasmaspheric quasi-periodic emissions as detected by the BBR onboard the DSX spacecraft. While a set of more typical QP emissions between 1 and 4 kHz were frequently detected, there was also the observation of higher frequency (5–15 kHz) QP emissions with episodes tending to occur at dawn and dusk and as the spacecraft extended to high magnetic latitudes. In some cases, the plasmaspheric density (as derived using the TNT-detected upper hybrid frequency) had a sharp gradient, with the density ranging from $<100/cm^3$ to >1000 cm^3 over the course of the episode. However, there were two noteworthy cases where the high frequency emissions remained outside a steep plasmaspheric density gradient – with the steepness of the gradient possibly determining access into the plasmasphere. We suggest the possibility that QP emission is created via density modulations that propagate through an equatorial source region. Recent work suggests that density modulations are common throughout the plasmasphere and such density modulations–especially quasi-periodic modulation–are capable of taking a wave-electron source into and out of resonance at the periodicity of the density wave. Next steps in this work include a ray tracing of the QP emissions, a more detailed development of a QP emission source (like that in Figure 11), and connecting the DSX QP emission set to those found by other spacecraft to thus place the new observations herein in context with preceding missions.

Data Availability Statement

The DSX data used to produce the figures can be accessed using https://doi.org/10.6084/m9.figshare.19070474.

Acknowledgments
We are very grateful from the support of the DSX project team and especially the operations team that kept the complex spacecraft flying successfully for 2 years. This work was supported by the Air Force Research Laboratory, and we want to also gratefully acknowledge the AFRL management team that provided resources for the mission and its extensions. The openness and sharing between the WPIx consortium partners, encouraged by its leadership team, has benefited the overall project and continues to be greatly appreciated. We also want to thank the BBR instrument development team for building such a robust and low noise flight system.

References

Bortnik, J., Li, W., Thorne, R. M., Angelopoulos, V., Cully, C., Bonnell, J., et al. (2009). An observation linking the origin of plasmaspheric hiss to discrete chorus emissions. *Science*, *324*(5928), 775–778. https://doi.org/10.1126/science.1171273

Bortnik, J., Thorne, R. M., & Meredith, N. P. (2008). The unexpected origin of plasmaspheric hiss from discrete chorus emissions. *Nature*, *452*(7183), 62–66. https://doi.org/10.1038/nature06741

Bortnik, J., Thorne, R. M., & Meredith, N. P. (2009). Plasmaspheric hiss overview and relation to chorus. *Journal of Atmospheric and Solar-Terrestrial Physics*, *71*(16), 1636–1646. https://doi.org/10.1016/j.jastp.2009.03.023

Coroniti, F. V., & Kennel, C. F. (1970). Electron precipitation pulsations. *Journal of Geophysical Research*, *75*(7), 1279–1289. https://doi.org/10.1029/ja075i007p01279

Demekhov, A. G., & Trakhtengerts, V. Y. (1994). A mechanism of formation of pulsating aurorea. *Journal of Geophysical Research*, *99*(A4), 5831–5841. https://doi.org/10.1029/93ja01804

Farrell, W. M., Morooka, M. W., Wahlund, J. E., Kurth, W. S., Hospodarsky, G., MacDowall, R. J., et al. (2017). Electromagnetic quasi-periodic whistler mode bursts during ring grazing passes. *American Geophysical Union. Fall Meeting 2017*, Abstract #SM33A-2637 Retrieved from https://ui.adsabs.harvard.edu/abs/2017AGUFMSM33A2637F/abstract

Gary, S. P., & Wang, J. (1996). Whistler instability: Electron anisotropy upper bound. *Journal of Geophysical Research*, *101*(A5), 10749–10754. https://doi.org/10.1029/96ja00323

Gurnett, D. A., & Bhattacharjee, A. (2005). *Introduction to plasma physics: With space and laboratory applications*, Cambridge Universtiy Press.

Hayosh, M., Němec, F., Santolík, O., & Parrot, M. (2014). Statistical investigation of VLF quasiperiodic emissions measured by the DEMETER spacecraft. *Journal of Geophysical Research: Space Physics*, *119*(10), 8063–8072. https://doi.org/10.1002/2013JA019731

Hayosh, M., Pasmanik, D. L., Demekhov, A. G., Santolik, O., Parrot, M., & Titova, E. E. (2013). Simultaneous observations of quasi-periodic ELF/VLF wave emissions and electron precipitation by DEMETER satellite: A case study. *Journal of Geophysical Research: Space Physics*, *118*(7), 4523–4533. https://doi.org/10.1002/jgra.50179

He, F., Guo, R. L., Guo, W. R. D., Yao, Z. H., Zhang, H. S., Hao, Y. X., et al. (2020). Plasmapause surface wave oscillates the magnetosphere and diffuse aurora. *Nature Communications*, *11*(1), 1668. https://doi.org/10.1038/s41467-020-15506-3

Hospodarsky, G. B., Imai, M., Kurth, W. S., Sulaiman, A. H., & Bolton, S. J. (2020). Juno waves observations of quasi-periodic (QP) emissions at Jupiter. *American Geophysical Union. Fall Meeting 2020*, abstract #SM057-06. Retrieved from https://ui.adsabs.harvard.edu/abs/2020AGUFMSM057.06H/abstract

Huang, X., Reinisch, B. W., Song, P., Green, J. L., & Gallagher, D. L. (2004). Developing an empirical density model of the plasmasphere using IMAGE/RPI observations. *Advances in Space Research*, *33*(6), 829–832. https://doi.org/10.1016/j.asr.2003.07.007

Johnston, W. R., Ginet, G. P., Su, Y.-J., Starks, M. J., McCollough, J. P., Sanchez, J. C., et al. (2022). Overview of the demonstration and science Experiments (DSX) mission. *Journal of Geophysical Research*. this issue.

LeDocq, M. J., Gurnett, D. A., & Anderson, R. R. (1994). Electron number density fluctuations near the plasmapause observed by the CRESS spacecraft. *Journal of Geophysical Research*, *99*(A12), 23661–23671. https://doi.org/10.1029/94ja02294

Linscott, I. R., Inan, U. S., Lauben, D. S., Farrell, W. M., Payne, J., Mossiwir, B., et al. (2022). The broad band receiver (BBR) payload. *Journal of Geophysical Research*, this issue.

Martinez-Calderon, C., Shiokawa, K., Miyoshi, Y., Keika, K., Ozaki, M., Schofield, I., et al. (2016). ELF/VLF wave propagation at subauroral latitudes: Conjugate observation between the ground and Van Allen Probes A. *Journal of Geophysical Research: Space Physics*, *121*(6), 5384–5393. https://doi.org/10.1002/2015JA022264

Martinez-Calderon, C., Shiokawa, K., Miyoshi, Y., Ozaki, M., Schofield, I., & Connors, M. (2015a). Polarization analysis of VLF/ELF waves observed at subauroral latitudes during the VLF-CHAIN campaign. *Earth Planets and Space*, *67*(1), 1–13. https://doi.org/10.1186/s40623-014-0178-7

Martinez-Calderon, C., Shiokawa, K., Miyoshi, Y., Ozaki, M., Schofield, I., & Connors, M. (2015b). Statistical study of ELF/VLF emissions at subauroral latitudes in Athabasca, Canada. *Journal of Geophysical Research: Space Physics*, *120*(10), 8455–8469. https://doi.org/10.1002/2015JA021347

Němec, F., Hospodarsky, G., Pickett, J. S., Santolik, O., Kurth, W. S., & Kletzing, C. (2016). Conjugate observations of quasiperiodic emissions by the cluster, Van Allen Probes, and THEMIS spacecraft. *Journal of Geophysical Research: Space Physics*, *121*(8), 7647–7663. https://doi.org/10.1002/2016JA022774

Němec, F., Hospodarsky, G. B., Bezdeˇková, B., Demekhov, A. G., Pasmanik, D., Santolík, O., et al. (2018). Quasiperiodic whistler mode emissions observed by the Van Allen Probes spacecraft. *Journal of Geophysical Research: Space Physics*, *123*(11), 8969–8982. https://doi.org/10.1029/2018JA026058

Němec, F., Pickett, J. S., & Santolík, O. (2014). Multispacecraft Cluster observations of quasiperiodic emissions close to the geo-magnetic equator. *Journal of Geophysical Research: Space Physics*, *119*(11), 9101–9112. https://doi.org/10.1002/2014JA020321

Němec, F., Santolík, O., Hospodarsky, G. B., Hajoš, M., Demekhov, A. G., Kurth, W. S., et al. (2020). Whistler mode quasiperiodic emissions: Contrasting Van Allen Probes and DEMETER occurrence rates. *Journal of Geophysical Research: Space Physics*, *125*(4), e2020JA027918. https://doi.org/10.1029/2020JA027918

Němec, F., Santolík, O., Pickett, J. S., Parrot, M., & Cornilleau-Wehrlin, N. (2013). Quasiperiodic emissions observed by the Cluster spacecraft and their association with ULF magnetic pulsations. *Journal of Geophysical Research: Space Physics*, *118*(7), 4210–4220. https://doi.org/10.1002/jgra.50406

Scherbarth, M., Smith, D., Adler, A., Stuart, J., & Ginet, G. (2009). AFRL's demonstration and science Experiments (DSX) mission. In S. Fineschi & J. A. Fennelly (Eds.), *Solar Physics and Space Weather Instrumentation III*. 74380B-10. https://doi.org/10.1117/12.824898

Schoenberg, J., Ginet, G., Dichter, B., Xapsos, M., Adler, A., Scherbarth, M., & Smith, D. (2006). *The demonstration and science Experiments (DSX): A fundamental science research mission advancing technologies that enable MEO spaceflight*. Defense Technical Information Center. #ADA464400. Retrieved from https://apps.dtic.mil/sti/citations/ADA464400

21699402, 2022, 8, Downloaded from https://agupubs.onlinelibrary.wiley.com/doi/10.1029/2022JA030327 by Koc University, Wiley Online Library on [03/11/2022]. See the Terms and Conditions (https://onlinelibrary.wiley.com/terms-and-conditions) on Wiley Online Library for rules of use; OA articles are governed by the applicable Creative Commons License